Vietnam Journal of Science and Technology ***59*** *(1) (2021) 120-134*

doi:10.15625/2525-2518/59/1/15261

NUMERICAL CALCULATION OF STATICALLY ADMISSIBLE SLIP-LINE FIELD FOR COMPRESSION OF A THREE-LAYER SYMMETRIC STRIP BETWEEN RIGID PLATES

Nguyen Manh Thanh[1, *], Nguyen Trung Kien[2], Sergei Alexandrov[3]

[1]*Institute of Mechanics, Vietnam Academy of Science and Technology, No.264 Doi Can Street, Ba Dinh District, Ha Noi, Viet Nam*

[2]*University of Communications and Transport, No.3 Cau Giay Street, Lang Thuong ward, Dong Da District, Ha Noi, Viet Nam*

[3]*Institute for Problems in Mechanics, Russian Academy of Sciences, Prospekt Vernadskogo, 101-1, Moscow 119526, Russia*

[*]Email: *manhthanh2012209@gmail.com*

Received: 10 July 2020; Accepted for publication: 27 December 2020

Abstract. This paper presents a method to build up statically admissible slip-line field and, as a result, the field of statically admissible stresses of plane-strain compression of a three-layer symmetric strip consisting of two different rigid perfectly plastic materials between rough, parallel, rigid plates The case is considered when the shear yield stress of the inner layer is greater than that of the outer layer. Under the conditions of sticking regime at bi-material interfaces and sliding occurs at rigid surfaces with maximum friction, the appropriate singularities on the boundary between the two materials have been assumed, then a standard numerical slip-line technique is supplemented with iterative procedure to calculate characteristic and stress fields that satisfy simultaneously the stress boundary conditions as well as the regime of sticking on the bi-material interfaces. The correctness of this admissible slip-line field model is confirmed by comparison with an analytical solution. It is shown that the singularities built at the end points of the line of separation of the materials are necessary to ensure the sticking regime on the interface of the strip layers.

Keywords: piece-wise homogeneous materials, rigid perfectly plastic materials, maximum friction surface, method of characteristics.

Classification numbers: 2.9.4, 5.4.5, 5.9.3.

1. INTRODUCTION

The problem of plane-strain compression of a strip between two parallel, rigid plates has a special position in plasticity theory. Starting from Prandtl-Nadai solution for rigid perfectly plastic material [1, 2], various analytical solutions, extended or generalized, for a strip of single material or piece-wise homogeneous materials have been given [3 - 6]. However, the corresponding numerical solutions have only been implemented for a strip of single rigid

perfectly plastic material, among which it is necessary to mention the solutions in [7-8] for stress and velocity and the solution for the distribution of the strain rate intensity factor along maximum friction surfaces [9]. These solutions were based on the theory of characteristics - also known as method of characteristics - due to the equations governing plastic flow in plane strain are hyperbolic and the characteristics for the stresses and the velocities coincide, furthermore, they coincide with the slip-lines for which the general theory is presented in [2, 10].

According to the analysis presented in [2, 8], a common to the problems of plane-strain compression of a strip between two parallel rigid plates is the presence of so-called rigid regions in the vicinity of overhanging parts, as well as in the center of the strip, where the elastic and plastic strains are of the same order, negligible compared to the plastic flow strains. The line of separation between rigid and plastic regions, which must be a slip line [8, 10], is not known in advance, moreover, their position often depends on the velocity boundary conditions. As a result, there are insufficient stress boundary conditions to define the slip-line field uniquely and thus the problem under consideration is not statically determined (Fig. 1a). The general approach to such problems must be a process of trial and error: a trial positions of rigid-plastic boundary are assumed, then associated slip-line fields, satisfying stress boundary conditions (also known as statically admissible slip-line fields) and corresponding velocity distribution are computed. Thus, uniqueness is obtained by choosing among statically admissible slip-line fields the one that also satisfies the velocity boundary conditions (Fig. 1b).

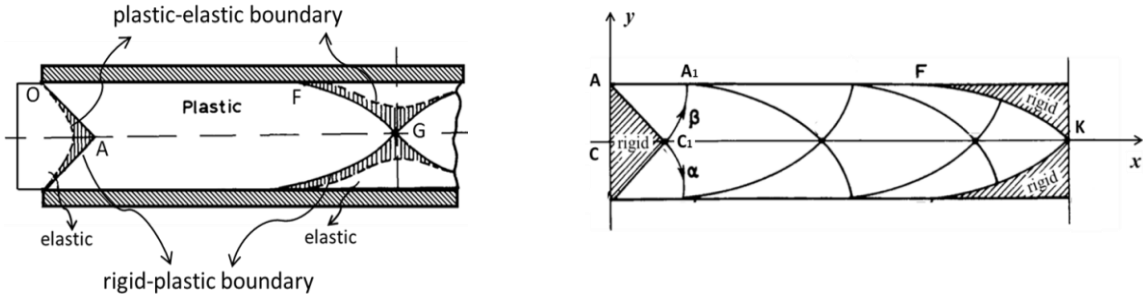

(a) (b)

Figure 1. Locations of the rigid and plastic areas in the compressed single strip.

This laborious process becomes even more complicated in the case of the compression of a multi-layer strip, when the field of statically admissible stresses must simultaneously satisfy the boundary conditions and the conditions of sticking regime at bi-material interfaces. In the present paper, as a first step to the development of a numerical method for calculating the stress and velocity fields in plane-strain flow of piece-wise homogeneous materials, the method of characteristics is used in the conjunction with the finite difference method to calculate statically admissible characteristic and stress fields for the problem formulated in [6], in the case of a three-layer symmetric strip, but without using simplified assumptions accepted in this paper.

2. BOUNDARY VALUE PROBLEM AND CONSTITUTIVE EQUATIONS

Consider a three-layer symmetric strip consisting of two different rigid perfectly plastic materials compressed between two parallel, rough, rigid plates. The thickness and width of the strip are $2H$ and $2L$, respectively. Denoting the inner and outer layers by the numbers 1 and 2, respectively, in parentheses, then, the shear yield stress and thickness of the outer layers will be

denoted by $k^{(2)}$ and $H^{(2)}$ respectively, and for the middle layer, by $k^{(1)}$ and $2H^{(1)}$. In addition, $H = H^{(1)} + H^{(2)}$. The plates are moving toward each other with speed U. A schematic diagram of the process and the Cartesian coordinate system (x, y) chosen are shown in Fig. 2. The maximum friction law occurs at $y = \pm H$. The end surfaces of overhanging parts of the strip are traction free.

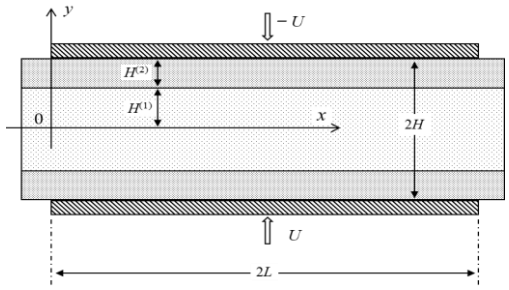

Figure 2. Configuration of the problem.

Let $\sigma_x^{(i)}$, $\sigma_y^{(i)}$, $\tau_{xy}^{(i)}$ and $v_x^{(i)}$, $v_y^{(i)}$ be the stress tensors and the velocity components respectively within the i-th layer (i = 1, 2). Because of symmetry, it is sufficient to consider the domain $0 \le x \le L$ and $0 \le y \le H$. In each layer where plastic flow occurs, the stress components satisfy the equilibrium equations and the plane-strain yield criterion while the velocity components are determined by the incompressibility and isotropy conditions. Since these systems are hyperbolic, there are two distinct characteristic directions at a point, denoted by α and β respectively. Substituting:

$$\sigma_y^{(i)},\ \sigma_x^{(i)} = \sigma^{(i)} \pm k^{(i)} \sin 2\varphi^{(i)} \quad , \quad \tau_{xy}^{(i)} = k^{(i)} \cos 2\varphi^{(i)} \tag{1}$$

here $\sigma^{(i)} = (\sigma_y^{(i)} + \sigma_x^{(i)})/2$ and $\varphi^{(i)}$ is the anti-clockwise angular rotation of the α-line from the x-axis in the i-th layer. It is known that the yield criterion is automatically satisfied by the stresses expressed in (1). Then, equations for α-lines and β-lines within each layer are

$$\frac{dy}{dx} = \tan\varphi^{(i)} \quad , \quad \frac{dy}{dx} = -\cot\varphi^{(i)}. \tag{2}$$

The α-line and β-line are regarded as right-handed curvilinear axes of reference, denoted by s_α and s_β respectively. Then, following [2, 10] in transforming from Cartesian coordinates (x, y) to the characteristic coordinates (s_α , s_β), with v_α and v_β being the components of the velocity vector along the characteristics, the equilibrium and velocity equations take the forms:

$$\sigma^{(i)} - 2k^{(i)}\varphi^{(i)} = constant \quad \text{on an } \alpha\text{-line} \tag{3}$$

$$\sigma^{(i)} + 2k^{(i)}\varphi^{(i)} = constant \quad \text{on a } \beta\text{-line} \tag{4}$$

$$dv_\alpha^{(i)} - v_\beta^{(i)} d\varphi^{(i)} = 0 \quad \text{along an } \alpha\text{-line} \tag{5}$$

$$dv_\beta^{(i)} + v_\alpha^{(i)} d\varphi^{(i)} = 0 \quad \text{along a } \beta\text{-line} \tag{6}$$

while the following boundary conditions hold (Fig. 2):

$$\varphi^{(1)} = -\frac{\pi}{4} \quad , \quad v_\alpha^{(1)} = v_\beta^{(1)} \quad \text{at} \quad y = 0 \tag{7}$$

$$\varphi^{(2)} = 0 \quad , \quad v_\beta^{(2)} = -U \quad \text{at} \quad y = H \tag{8}$$

Due to the condition of sticking, the both normal and tangent velocity components as well as the normal and shear stress are continuous across bi-material interfaces. This leads to:

$$\sigma^{(1)} + k^{(1)} \sin 2\varphi^{(1)} = \sigma^{(2)} + k^{(2)} \sin 2\varphi^{(2)} \tag{9}$$

$$k^{(1)} \cos 2\varphi^{(1)} = k^{(2)} \cos 2\varphi^{(2)} \tag{10}$$

$$v_\alpha^{(1)} \cos\varphi^{(1)} - v_\beta^{(1)} \sin\varphi^{(1)} = v_\alpha^{(2)} \cos\varphi^{(2)} - v_\beta^{(2)} \sin\varphi^{(2)} \tag{11}$$

$$v_\alpha^{(1)} \sin\varphi^{(1)} + v_\beta^{(1)} \cos\varphi^{(1)} = v_\alpha^{(2)} \sin\varphi^{(2)} + v_\beta^{(2)} \cos\varphi^{(2)} \tag{12}$$

So, in each layer there are six equations (3), (4), (5), (6) and (2) for determining six unknowns $\sigma_y^{(i)}$, $\sigma_x^{(i)}$, $v_x^{(i)}$, $v_y^{(i)}$ and the Cartesian coordinates x, y of an nodal points of the computational grid created by slip-line families α and β. To calculate the unknowns on bi-material interface $y = H^{(1)}$, four conditions of continuity (9), (10), (11) and (12) must be added to the group of the mentioned equations. Regarding the task of determining the field of statically admissible stresses, it was enough to use six equations (2), (3), (4), (9), (10) for the points at the interface of two materials and four equations (2), (3), (4) for remaining points of the strip.

3. COMPATIBILITY OF VELOCITY COMPONENTS AT THE END POINTS OF BI-MATERIAL INTERFACE

In order to create a numerical scheme for developing a statically admissible stress field in a compressed strip, it is necessary to clarify the kinematic conditions at rigid-plastic boundaries, regardless of whether the strip under consideration is single or multi-layer.

Consider, for example, the general structure of the slip-line field found in [8]. The material at the edge of the strip to the left of the α-line AC_1, which is also a rigid-plastic boundary, move outward as a rigid body. The rigid area at the center of the strip is moved down with the rigid plate, losing material to the plastic region to the left of the rigid-plastic boundary, α-line FK. Since the first of these regions contains the symmetric line $y = 0$, its velocity component v_y is equal to zero, and the incompressibility condition dictates that its component v_x is equal to $-U_1$, here $U_1 = U.L/H$. Similarly, the components of the velocity v_x and v_y for a rigid region in the center of the strip that contains the symmetric line $x = 0$ will be zero and $-U$, respectively (Fig. 3). Therefore, the velocity components v_α^R, v_β^R of the rigid regions along rigid-plastic boundaries are

$$v_\alpha^R = -U \sin\varphi \quad , \quad v_\beta^R = -U \cos\varphi \quad \text{along } FK \tag{13}$$

$$v_\alpha^R = -U_1 \cos\varphi \quad , \quad v_\beta^R = U_1 \sin\varphi \quad \text{along } AC_1 \tag{14}$$

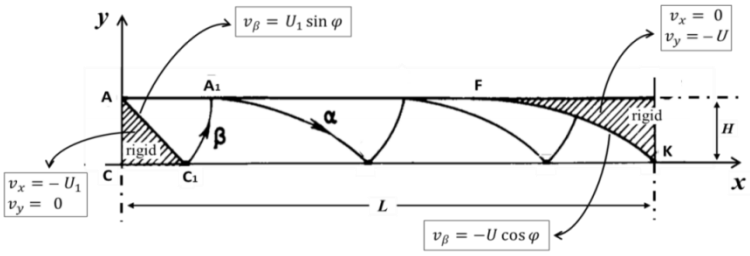

Figure 3. General structure of the slip-line field in compressed single strip.

Using (5), (7) and taking into account that the normal velocity component v_β must be continuity across rigid-plastic boundary, the velocity components of the plastic region along the rigid-plastic boundary *FK* are determined as

$$v_\alpha = -U(\sqrt{2} + \sin\varphi)\ , \quad v_\beta = -U\cos\varphi \quad \text{along } FK \tag{15}$$

Now, for the case of the strip shown in Fig. 2, the structure of the slip-line field will change. The slip-lines of the same family (α or β) obviously intersect the line $y = H^{(1)}$ at different angles $\varphi^{(1)}$and $\varphi^{(2)}$, for which relation (10) is satisfied, as shown in Fig. 4 for a rigid-plastic boundary passing piece-wise smoothly through the points *F*, *G*, *K*. For the inner layer, due to the presence of the condition (7), relations (15) remain valid, while for the outer layer, only the second equality from (15) is satisfied. Thus

$$v_\beta^{(2)} = -U\cos\varphi^{(2)} \quad \text{along the } \alpha\text{-line } FG \tag{16}$$

$$v_\alpha^{(1)} = -U\left(\sqrt{2} + \sin\varphi^{(1)}\right)\ , \quad v_\beta^{(1)} = -U\cos\varphi^{(1)} \quad \text{along the } \alpha\text{-line } GK \tag{17}$$

Using these just obtained kinematic relations and also the continuity conditions (11) and (12), the following fact was proved

$$\sin\left(\varphi_G^{(1)} - \varphi_G^{(2)}\right) = 0 \quad \text{at the point } G \tag{18}$$

where $\varphi_G^{(1)}$ and $\varphi_G^{(2)}$ are the values of the functions $\varphi^{(1)}$ and $\varphi^{(2)}$ respectively at *G*, the intersection of the rigid-plastic boundary *FK* with the line of separation between the two materials. Comparing (10) and (18) shows that

$$\varphi_G^{(1)} = \varphi_G^{(2)} = -\pi/4 \quad \text{if} \quad k^{(1)} \neq k^{(2)} \tag{19}$$

This conclusion means that the rigid-plastic boundary must always cross the line of separation of the two materials at an angle of $-\pi/4$. This seems unrealistic and, moreover, it will lead to obvious contradictions when we change the input parameters $k^{(1)}$, $k^{(2)}, H^{(1)}, H^{(2)}$in such a way that the ratio $(k^{(2)}/k^{(1)})$ approaches asymptotically to 1, while the ratio $(H^{(2)}/H^{(1)})$ approaches zero. In this way, we will approach the model of single-layer strip compressed between rough, parallel, rigid plates but with a zero shear stress at the friction surfaces. The same situation also occurs at the points of intersection between the line $y = H^{(1)}$ and the rigid-plastic boundary at the outer edges of the strip. Thus, there are incompatibilities of the velocity components at the intersection of the boundaries under consideration.

In order to escape the absurd situation presented above, an assumption of the existence of a singularity at the end intersection points on the line of separation of the materials is proposed in the following section.

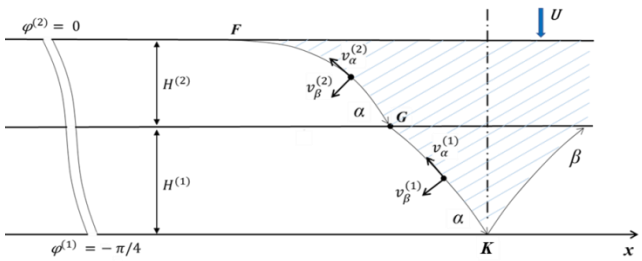

Figure 4. A piece-wise smooth boundary between rigid and plastic region.

4. CONFIGURATION OF AN ASSUMED FIELD OF THE CHARACTERISTICS

4.1. General description

The configuration of an assumed field of the slip-lines and Cartesian coordinates (*x*, *y*) for a three-layer symmetric strip, with slip-lines *ADP* and *FGK* being rigid-plastic boundaries, are symbolically illustrated in Fig. 5. The point *A* is a singularity through which pass all α-lines within an angle θ between the two straight slip-lines AA_1, *AD*. The β-line through *A* is degenerated into point *A*. Thus, the β-line DA_1 is circular arc with it center in point *A*. The value of the angle θ, created by the segment *AD* with the *x*-axis (i.e $\theta = \varphi_A^{(2)} = \varphi_D^{(2)}$), is also assumed and will be determined from the overall solution of the problem. Within the inner layer, the segment *DP* is assumed to be a straight line and form with *x*-axis of an angle equal to $-\pi/4$. According to [8], the segment A_1F is not an α-line but an envelope of α-lines. In addition to the singular point *A*, there are also singularities at points *G*, *D*.

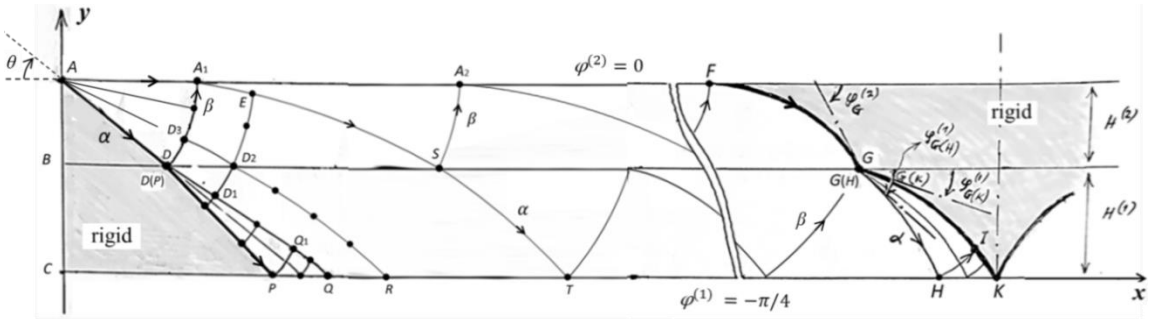

Figure 5. General structure of of an assumed slip-line field.

Suppose that *G* and *D* are the singular points for the inner layer. This implies the existence of an angle $\varphi_{G(K)}^{(1)}$ such that in the interval $\{\varphi_{G(H)}^{(1)}; \varphi_{G(K)}^{(1)}\}$ the β-line that passes *G* is a degenerate characteristic and all α-lines of the inner layer converging in *G* form a centered fan. The notations *G*(*H*) and *G*(*K*) used for the start and end points of a degenerate β-line, respectively, means that the α-lines originating from these points will intersect the *x*-axis at points *H* and *K*, respectively. Obviously, these two points have the same Cartesian coordinates as point *G*. The same is true for the singularity at point *D*, where the degenerate β-line passes through points *D*(*P*) and *D*(*Q*). The angles between α-lines *D*(*P*)*P*, *D*(*Q*)*Q* and the *x*-axis at the points *D*(*P*), *D*(*Q*) will be noted by $\varphi_{D(P)}^{(1)}$and $\varphi_{D(Q)}^{(1)}$ respectively, where $\varphi_{D(P)}^{(1)} = -\pi/4$ according to the assumption given above. An another configuration with a curved segment *DP* can be considered but, for the task of constructing an statically admissible stresse field, the numerical scheme remains unchanged. Therefore, in the next presentation, we will consider only the case described in figure 5.

4.2. Necessary conditions on rigid-plastic boundaries

4.2.1. Kinematic condition at the point G

Regarding the angles $\varphi_{G(K)}^{(1)}$ and $\varphi_{D(Q)}^{(1)}$ mentioned above, it should be emphasized that the

value of angle $\varphi_{D(Q)}^{(1)}$ can be calculated immediately using the expression (10), while the value of angle $\varphi_{G(K)}^{(1)}$ can only be determined at the end of the construction of slip-line field, when the outer α-line reaches the position of the rigid-plastic boundary *FGK*.

Since the α-lines *FG* and *G*(*K*)*K* form the boundary between the plastic and rigid zones by assumption, the kinematic conditions (16) for segment *FG* and (17) for segment *G*(*K*)*K* must be satisfied. In particular, at the point *G* for the outer layer, (17) take the form:

$$v_{\beta|G}^{(2)} = -U\cos\varphi_G^{(2)} \tag{20}$$

At the same time, the continuity conditions of the normal and tangent velocity components at bi-material interface y = $H^{(1)}$ require that at the point *G*(*H*) be satisfied:

$$v_{\beta|G}^{(2)} = -v_{x|G(H)}.\sin\varphi_G^{(2)} + v_{y|G(H)}.\cos\varphi_G^{(2)} \tag{21}$$

or, taking into account (20), after simple conversions:

$$-U\cos\varphi_G^{(2)} = v_{\alpha|G(H)}^{(1)}.\sin\left(\varphi_{G(H)}^{(1)} - \varphi_G^{(2)}\right) + v_{\beta|G(H)}^{(1)}.\cos\left(\varphi_{G(H)}^{(1)} - \varphi_G^{(2)}\right) \tag{22}$$

Obviously, in addition to the location of the point G, the position and shape of the α-line passing the points *G*(*K*), *I*, *K* also depend on the angle $\varphi_{G(K)}^{(1)}$ at point *G*(*K*) and the stress data obtained on the α-line *G*(*H*)*H*. Based on formulas (17) and the boundary condition (7), the velocity components $v_\alpha^{(1)}$, $v_\beta^{(1)}$ in the regions *HIK* and *G*(*H*)*G(K)IH* (i.e *GHI*) can be calculated using the numerical procedure proposed in [2]. The velocity values $v_{\alpha|G(H)}^{(1)}$ and $v_{\beta|G(H)}^{(1)}$ obtained at point *G*(*H*) must satisfy the condition (22). The task now is as follows:

Find the position of the point G on the two-material interface and such a value of the angle $\varphi_{G(K)}^{(1)}$ *so that the conditions* (22) *and* (*x*(*K*) = *L*) *are simultaneously satisfied*.

Next, the suitable stress boundary conditions should be set on the rigid-plastic boundary *ADP*. Since the angles $\varphi^{(1)}$ and $\varphi^{(2)}$ on *AD* and *D*(*P*)*P* are already known by assumption, it is necessary to determine only the distributions of $\sigma^{(1)}$ and $\sigma^{(2)}$ on these segments.

4.2.2 Condition for the stresses on the line ADP

Using equation (3) for point *D*, equation (4) for the points *D*(*P*), *D*(*Q*) and taking into account the continuity conditions (9), (10) at the point *D*(*Q*), the relation between the constants on *AD* and *D*(*P*)*D*(*Q*) is determined as

$$\sigma_{\beta[D(P)D(Q)]}^{(1)} = \sigma_{\alpha[AD]}^{(2)} + \mathcal{F}\left(k^{(1)}, k^{(2)}, \theta\right) \tag{23}$$

here $\sigma_{\alpha[AD]}^{(2)}$ is the constant in (10) for α-line *AD* and $\sigma_{\beta[D(P)D(Q)]}^{(1)}$ is the constant in (11) for degenerate β-line *D*(*P*)*D*(*Q*). The expression of the function $\mathcal{F}\left(k^{(1)}, k^{(2)}, \theta\right)$ is

$$\mathcal{F}\left(k^{(1)}, k^{(2)}, \theta\right) = \left[2k^{(2)}\theta + 2k^{(1)}\varphi_{D(Q)}^{(1)} + k^{(2)}\sin 2\theta - k^{(1)}\sin 2\varphi_{D(Q)}^{(1)}\right] \tag{24}$$

Thus, the value of $\sigma^{(1)}$ and $\sigma^{(2)}$ at the points *D*(*P*) and *D*, respectively, are

$$\sigma_{D(P)}^{(1)} = k^{(1)}\left(\frac{\pi}{2}\right) + \mathcal{F}\left(k^{(1)}, k^{(2)}, \theta\right) + \sigma_{\alpha[AD]}^{(2)} \tag{25}$$

$$\sigma_D^{(2)} = 2k^{(2)}\varphi_D^{(2)} + \sigma_{\alpha[AD]}^{(2)} = 2k^{(2)}\theta + \sigma_{\alpha[AD]}^{(2)} \tag{26}$$

Since the values of the angles $\varphi^{(1)}$ and $\varphi^{(2)}$ are constant on the segments *D*(*P*)*P* and *AD*, respectively, the values of $\sigma^{(1)}$ and $\sigma^{(2)}$ are also constant on these segments.

Using (25), (26) and the expression (1) for the component $\sigma_x^{(i)}$, the force acting in the *x*-direction on the segments *D*(*P*)*P* and *AD* from the side of the plastic region is determined as

$$F_x = k^{(1)}H^{(1)}\left(\frac{\pi}{2}+1\right) + H^{(1)}\mathcal{F}\left(k^{(1)},k^{(2)},\theta\right) + k^{(2)}H^{(2)}(2\theta - \sin 2\theta) + \left(H^{(1)}+H^{(2)}\right)\sigma_{\alpha[AD]}^{(2)} \tag{27}$$

Since the end surfaces of overhanging part of the strip are traction free, the equilibrium condition of the rigid portion *ADPCB* requires that force *Fx* must equal zero. That yield

$$\sigma_{\alpha[AD]}^{(2)} = -\frac{k^{(1)}H^{(1)}\left(\frac{\pi}{2}+1\right) + H^{(1)}\mathcal{F}\left(k^{(1)},k^{(2)},\theta\right) + k^{(2)}H^{(2)}(2\theta - \sin 2\theta)}{\left(H^{(1)}+H^{(2)}\right)} \tag{28}$$

Thus, all stress boundary conditions have been defined on the rigid-plastic boundary *ADP*.

5. NUMERICAL SOLUTION

5.1. Numerical scheme

Several numerical schemes based on the method of characteristics have been proposed to determine the stress and velocity distributions in plane-strain flow of rigid perfectly single plastic strip compressed between two parallel, rough, rigid plates [2, 7, 8]. In the present paper we adopt the classical scheme presented in [8], with appropriate modification, to solve the problem formulated in the section 2.

Consider general structure of of the slip-line field shown in Fig. 5. Starting from base-line *ADP*, the stress distribution across a network of characteristics (slip-lines) can be uniquely defined by the systems (2), (3), (4) and the boundary conditions (7), (8).

5.1.1. Construction of the slip-line field in the regions AA_1D and DQP

Since α-lines are straight in the regions AA_1D and DQ_1P while β-lines DA_1 and PQ_1 are circular arcs with their centers in the points *A* and *D*, respectively, the distribution of the quantities φ and σ is automatically determined by the values of these quantities on any of the circular slip lines, no numerical treatment is required in these regions [2, 10]. In fact, having the constant value $\sigma_{\alpha[AD]}^{(2)}$ in (28), the constant $\sigma_{\beta[DA_1]}^{(2)}$ for β-line DA_1 is immediately calculated by using the value $\sigma_D^{(2)}$ in (26) and equation (4) for β-line DA_1

$$\sigma_{\beta[DA_1]}^{(2)} = 4k^{(2)}\theta + \sigma_{\alpha[AD]}^{(2)} \tag{29}$$

Thus, the distribution of $\sigma_{DA_1}^{(2)}$ on β-line DA_1 is

$$\sigma_{DA_1}^{(2)} = -2k^{(2)}\varphi_{DA_1}^{(2)} + 4k^{(2)}\theta + \sigma_{\alpha[AD]}^{(2)} \tag{30}$$

Similarly, the distribution of $\sigma_{D(P)D(Q)}^{(1)}$ on degenerate β-line *D*(*P*)*D*(*Q*) is

$$\sigma^{(1)}_{D(P)D(Q)} = -2k^{(1)}\varphi^{(1)}_{D(P)D(Q)} + \mathcal{F}\left(k^{(1)}, k^{(2)}, \theta\right) + \sigma^{(2)}_{\alpha[AD]} \tag{31}$$

It follow from (31), when $\varphi^{(1)}_{PQ_1}$ varies in the interval $\{-\pi/4\,;\, \varphi^{(1)}_{D(Q)}\}$ on β-line PQ_1, the distribution of $\sigma^{(1)}_{PQ_1}$ is

$$\sigma^{(1)}_{PQ_1} = -2k^{(1)}\varphi^{(1)}_{PQ_1} + \mathcal{F}\left(k^{(1)}, k^{(2)}, \theta\right) + \sigma^{(2)}_{\alpha[AD]} \tag{32}$$

Next, having the distribution of $\sigma^{(1)}_{PQ_1}$, $\varphi^{(1)}_{PQ_1}$ and the boundary conditions (7), the stress distribution and slip-line field in the region PQ_1Q is defined by the numerical procedure described in [2] and, as a result, all necessary stress boundary conditions have been defined on the β-line DA_1 and the α-line DQ (i.e $D(Q)Q$). Now, the full set of known boundary conditions on the segments DA_1 and DQ can be rewritten by the following relations

$$y^{(2)} = y^{(2)}_{DA_1}(x)\ ,\ \ \sigma^{(2)} = \sigma^{(2)}_{DA_1}(x)\ ,\ \ \varphi^{(2)} = \varphi^{(2)}_{DA_1}(x) \quad \text{on } DA_1 \tag{33}$$

$$y^{(1)} = y^{(1)}_{DQ}(x)\ ,\ \ \sigma^{(1)} = \sigma^{(1)}_{DQ}(x)\ ,\ \ \varphi^{(1)} = \varphi^{(1)}_{DQ}(x) \quad \text{on } DQ \tag{34}$$

here, all functions in (33) and (34) are considered to be given. Thus, instead of the rigid-plastic boundary *ADP*, the segments DA_1 and *DQ* become starting lines for the construction of slip-line field to the right of these segments. Since the boundary values for each layer of the strip were not given on the line $y = H^{(1)}$, a special procedure taking into account the sticking regime must be established to determine the unknowns on this line.

5.1.2. Construction of the field in region surrounded by multi-segment line DA_1FGHQ

Consider the segment *DQ* now divided into *N* smaller segments by nodal points. The next after point *D* is D_1, given by the boundary values x_{D_1}, $y^{(1)}_{D_1}$, $\varphi^{(1)}_{D_1}$, $\sigma^{(1)}_{D_1}$ satisfying the conditions

$$y^{(1)}_{D_1} = y^{(1)}_{DQ}\left(x_{D_1}\right)\ \ ,\ \ \varphi^{(1)}_{D_1} = \varphi^{(1)}_{DQ}\left(x_{D_1}\right)\ \ ,\ \ \sigma^{(1)}_{D_1} = \sigma^{(1)}_{DQ}\left(x_{D_1}\right) \tag{35}$$

Then the point D_2 on the line $y = H^{(1)}$ through which the β-line originating from D_1 passes, and the point D_3 on the segment DA_1 through which the α-line originating from D_2 passes, are determined by non-linear system of six equations (2), (3), (4), (9), (10) in finite-difference form for the six unknown denoted by the vector symbol $\bar{\boldsymbol{X}}$

$$\bar{\boldsymbol{X}} \equiv \{X_1, X_2, X_3, X_4, X_5, X_6\}^T \equiv \{\sigma^{(2)}_{D_2},\ \sigma^{(1)}_{D_2},\ x_{D_2},\ x_{D_3},\ \varphi^{(2)}_{D_2},\ \varphi^{(1)}_{D_2}\}^T \tag{36}$$

$$-X_1 + 2k^{(2)}X_5 + \sigma^{(2)}_{DA_1}(X_4) - 2k^{(2)}\varphi^{(2)}_{DA_1}(X_4) = 0 \tag{37}$$

$$-X_2 - 2k^{(1)}X_6 + \sigma^{(1)}_{D_1} - 2k^{(1)}\varphi^{(1)}_{D_1} = 0 \tag{38}$$

$$(X_3 - X_4)\tan\left(\frac{\varphi^{(2)}_{DA_1}(X_4) + X_5}{2}\right) + y^{(2)}_{DA_1}(X_4) - H^{(1)} = 0 \tag{39}$$

$$\left(x_{D_1} - X_3\right)\tan\left(\frac{\varphi^{(1)}_{D_1} + X_6}{2}\right) + y^{(1)}_{D_1} - H^{(1)} = 0 \tag{40}$$

$$X_1 - X_2 + k^{(2)}\sin 2X_5 - k^{(1)}\sin 2X_6 = 0 \tag{41}$$

$$k^{(2)} \cos 2X_5 \; - \; k^{(1)} \cos 2X_6 \;\; = \; 0 \tag{42}$$

As a rule, this non-linear system is solved by iterative gradient method.

Now, starting from D_2, all nodes on the β-line from D_2 to E as well as on the α-line from D_2 to R are defined by the numerical procedure proposed in [2]. Having all necessary stress boundary conditions on the segments D_2E and D_2R and acting in a similar way, all the nodal points and, consequently, the slip-line field in the region surrounded by the segments D_2E, ES, ST, TR and RD_2 are determined. Next, the field in region A_1A_2S is defined by the solutions on A_1S and the boundary condition (8).

Thus, with the solutions obtained on the β-line SA_2 and on the α-line ST, the segments SA_2 and ST now become starting lines for the construction of slip-line field for the plastic region to the right of these segments. In a similar way, the construction of the field continues to the α-line that passes through such a point H, located near and to the left of the point K on the x-axis. This α-line intersects the lines $y = H^{(1)}$ and $y = H$ at points G and F, respectively. The segment FG is temporarily considered to be part of the rigid-plastic boundary. At this moment, it is not clear whether this temporarily viewed as a rigid-plastic boundary intersects with the x-axis at point K.

5.1.3. Construction of the field in the region GHK

The process of finding the location of the point G and the value of the angle $\varphi^{(1)}_{G(K)}$, which meet the requirements specified in paragraph 4.2.1, is carried out in two phases: first, it is necessary to define only the angle $\varphi^{(1)}_{G(K)}$, which satisfies the condition (22), while the location of point G is preselected intuitively as described above.Then, the location of the point G is adjusted according to the iterative procedure so that coordinate $x(K)$ approach to the value of L.

First of all, one value for the angle $\varphi^{(1)}_{G(K)}$ is chosen so that the following condition is met

$$\varphi^{(1)}_{G(H)} \; < \; \varphi^{(1)}_{G(K)} \; < \; 0 \tag{43}$$

Consider the degenerate segment $G(H)G(K)$, now divided into smaller segments by $(M + 1)$ equally spaced nodal points, among which $G(H)$ and $G(K)$ are the first and last in order, respectively. So, these points have the same Cartesian coordinates, while the value of the angle $\varphi^{(1)}$ of two successive points is equal to $(\varphi^{(1)}_{G(K)} - \varphi^{(1)}_{G(H)})/M$. Then, using the known values of $\varphi^{(1)}$ and $\sigma^{(1)}$ at $G(H)$, the quantity $\sigma^{(1)}$ at the remaining points on $G(H)G(K)$ is calculated according to (4). Using boundary condition (7) and the data just received on $G(H)G(K)$ along with the one on the α-line $G(H)H$, the slip-line field in the region $G(H)G(K)IKH$ is defined by the known procedure mentioned in [2].

Next, starting from temporarily considered as rigid-plastic boundary $G(K)K$ and taking into account the conditions (17), (7), the velocity components $v^{(1)}_{\alpha}$, $v^{(1)}_{\beta}$ in the region $G(H)G(K)IKH$ can be found using the equations (5), (6) in finite-difference form.

Now, having the velocity solutions at the point $G(H)$, one suitable iterative gradient method is used for the determination of the value of $\varphi^{(1)}_{G(K)}$, which meet the condition (30). For this purpose, substituting $\varphi^{(1)}_{G(K)}$ by symbol X, the condition (22) is rewritten in the form

$$\mathcal{F}(X) = v^{(1)}_{\alpha|G(H)}.\sin\left(\varphi^{(1)}_{G(H)} - \varphi^{(2)}_{G}\right) \; + \; v^{(1)}_{\beta|G(H)}.\cos\left(\varphi^{(1)}_{G(H)} - \varphi^{(2)}_{G}\right) + U.\cos\varphi^{(2)}_{G} = 0 \tag{44}$$

According to the gradient method, the solution of the equation (44) will be the minimum point of the function $\Psi(X) = \left(\mathcal{F}(X)\right)^2$ when using the iterative procedure:

$$X^{(n+1)} = X^{(n)} - \alpha_n \cdot \frac{\boldsymbol{\nabla}\Psi\left(X^{(n)}\right)}{\|\boldsymbol{\nabla}\Psi(X^{(n)})\|} \tag{45}$$

here $\frac{\boldsymbol{\nabla}\Psi\left(X^{(n)}\right)}{\|\boldsymbol{\nabla}\Psi(X^{(n)})\|}$ is the unit gradient vector of $\Psi(X)$ at $X^{(n)}$, $X^{(0)}$ is the value of $\varphi^{(1)}_{G(K)}$ chosen above, α_n is the value of the gradient step. In addition, $X^{(n)}$ must satisfy the condition (43) for all values of *n*. Then, using the value of $\varphi^{(1)}_{G(K)}$ which is the solution of (44), we will get the slip-line field in region *G*(*H*)*G(K)IKH* that meets the condition (22).

Thus, with preselected coordinate value *x*(*G*), the value *x*(*K*) is defined at the end of the first phase. Suppose that the relationship between the quantities *x*(*G*) and (*x*(*K*) - *L*) is one-to-one and is expressed by the function $\mathcal{F}_G(X) = \mathcal{F}_G(x(G)) = x(K) - L$. Then, the coordinate value *x*(*G*) is determined by an iterative procedure similar to the procedure (45) described above.

5.2. Numerical results and comparison

Consider an analytic solution to the problem formulated in section 2, in which the boundary conditions at $x = 0$ and $x = L$ are ignored, while all the equations and the boundary conditions at $y = H$ as well as the conditions of sticking regime at $y = H^{(1)}$ are satisfied [6]. Since this solution gives a good approximation to the solution for the problem under consideration, except near the ends and center of the strip, it is inferred that it is appropriate to be used to evaluate numerical results obtained here if the width of the strip is large enough compared to its thickness.

It should be noted that in numerical scheme presented above, the solutions for each layer are first calculated for nodes at bi-material interface, then they are separately used as boundary conditions for calculating solutions inside each layer by already known numerical method used for solving the problem of compressing a single layer strip. Therefore, the solution for nodes inside each layer will depend mainly on the solution for that layer on the segment *DG*. For this reason, we only need to compare the numerical results and analytical solution on this segment.

The calculations were performed for strips with the ratios $k^{(1)}/k^{(2)}$ in the range of {1.1→ 7.9}, *L*/*H* in the range of {8 →14}, $H^{(1)}/H^{(2)}$ in the range of {0.8→ 2.5} and an angle θ in the range of {-0.77 → -0.3}. Without loss of generality, it is assumed that $H = 1.5$ and $k^{(2)} = 1$ in all calculations.

The volume of calculations mainly falls on the solution of the nonlinear system of equations (37) – (42) for nodes at bi-material interface *DG* by the iterative method. The criterion for stopping the iterative process is: $\left\|\overline{\boldsymbol{X}}^{(n+1)} - \overline{\boldsymbol{X}}^{(n)}\right\| = \max_{i=1\div6}\left|X_i^{(n+1)} - X_i^{(n)}\right| \le \varepsilon_{DG} = 10^{-4}$. The actual calculation process shows that the number of iterations *n* for nodes on segment *DG* ranges from 50 ÷ 70 depending on factors such as input parameters $\{k^{(i)}, H^{(i)}\}$ and the choice of the initial approximation vector $\overline{\boldsymbol{X}}^{(0)}$ for each node on this segment. Such a fairly large number of iterations shows that the algorithm set up in computation program is not yet optimal, but in return, convergence is guaranteed when the input parameters change over a wide range.

Figure 6 shows the three slip-line field configurations corresponding to three set of calculation parameters in which the results for quantities *x*(*G*), $\varphi^{(2)}_G$, $\varphi^{(1)}_{G(H)}$ and $\varphi^{(1)}_{G(K)}$ are described. In all cases, the number of nodes (*N* + 1) on the segment *DQ* are equal to 26. The pink lines represent the family of α-lines, while the β-line family is shown in blue. The slip-line field in region ADA_1 was calculated in the classical way and therefore is not displayed in the figures.

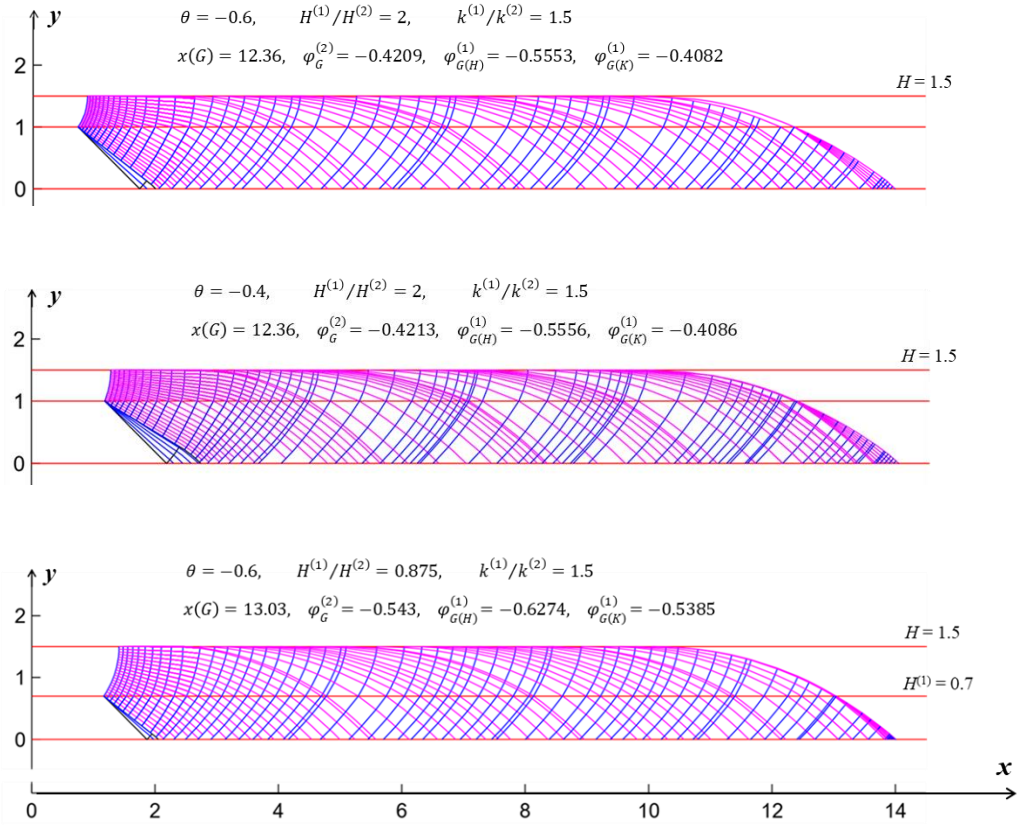

Figure 6. Slip-line fields calculated for strips of different set of calculation parameters.

Next, for each of the two sets of input parameters, when the angle θ takes values equal to -0.4, -0.5, -0.6, and -0.7, respectively, the normal and shear stress distributions on the segment *DG* for the numerical results and analytical solutions are compared on the four graphs. Figure 7 shows the first case with ratios: $H^{(1)}/H^{(2)} = 2$, $k^{(1)}/k^{(2)} = 1.5$. The second case, with ratios: $H^{(1)}/H^{(2)} = 0.875$, $k^{(1)}/k^{(2)} = 3$, is shown in Fig. 8. The ratio $L/H = 9.33$ for both cases. On the vertical axis of the plots are dimensionless values of stresses

$$\bar{\sigma}_x^{(1)} = \sigma_x^{(1)}/k^{(2)}, \quad \bar{\sigma}_x^{(2)} = \sigma_x^{(2)}/k^{(2)}, \quad \bar{\sigma}_y^{(i)} = \sigma_y^{(i)}/k^{(2)}, \quad \bar{\tau}_{xy}^{(i)} = \tau_{xy}^{(i)}/k^{(2)}$$

Comparison of these graphs leads to the following remarks:

a) When the variable x lies in the distances greater than $2H$ from the edge of the plate, the numerical and analytical values vary in the same way (their derivatives are equal) and they differ from each other only by constants called the constants of the statically admissible field under consideration.

b) The mentioned above constants vary depending on the value of the angle θ, so θ is the determining parameter of the configuration of an assumed slip-line field.

In the area near the edge of the strip, the solutions will naturally be highly influenced by the stress boundary conditions at the surface $x = 0$. Since the exact boundary conditions for $\sigma_x^{(i)}$, $\tau_{xy}^{(i)}$ at $x = 0$ have been replaced by only one approximate relation $\int_0^H \sigma_x dy = 0$ in [6], then noticeable discrepancies at different values of θ between the numerical and analytical solutions in region $x < 2H$ are inevitable.

Interestingly, for $x > 2H$ and regardless of θ, there was an almost complete similarity of numerical and analytical results for the quantities $\tau_{xy}^{(i)}$. This is due to the characteristic behavior of $\sigma_x^{(i)}$ noted in remark a) and the fact that in the mentioned range, the shear stress becomes independent of the change in x. In fact, consider an α-line that intersects the segments AF and DG at points A' and D', respectively and check the equilibrium condition in the x-direction for the region $A'FGD'$. Then, it follows from remark a) that the resulting forces in the x-direction on the segments $A'D'$ and FG for the analytical and numerical models become equal to each other as soon as the point D' falls into the zone $x > 2H$. As a result, the resulting forces in this direction on the segments $A'F$ and $D'G$ for both models are also equal to each other. Since both models have the same boundary condition on $A'F$, the force components in the x-direction for them on $D'G$ must be equal to each other. Hence the equality of shear stresses $\tau_{xy}^{(i)}$ is followed, since they do not change within the considered range.

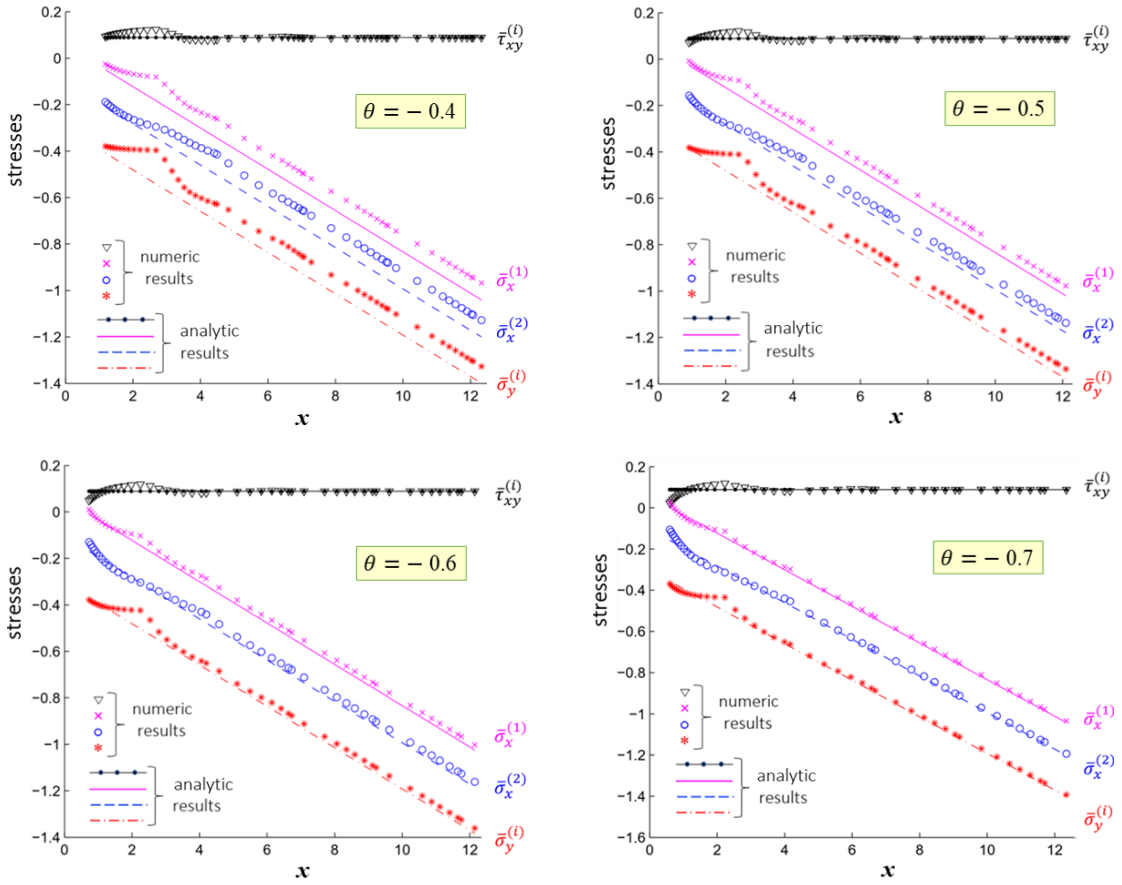

Figure 7. Comparison of numeric and analytic values of $\bar{\sigma}_x^{(1)}$, $\bar{\sigma}_x^{(2)}$, $\bar{\sigma}_y^{(i)}$, $\bar{\tau}_{xy}^{(i)}$ on segment DG (The case: $H^{(1)}/H^{(2)} = 2$, $k^{(1)}/k^{(2)} = 1.5$).

Obviously, in a configuration where the segment DP is curved, along with the angle θ, the coordinates at its nodes will be the determining parameters of the configuration. Thus, the correct solutions to the boundary-value problem can be obtained using a process in which these parameters are adjusted so that the constants of the admissible field approaching zero and in this way, the main meaning of the admissible fields obtained here is confirmed.

Perhaps, there is also a case where the obtained solution of equation (44) does not satisfy condition (43). This means that the angle value θ chosen for the configuration was not suitable for a given set of input parameters $\{k^{(i)}, H^{(i)}\}$. The extreme case, when such suitable value of the angle θ do not exist, corresponds to the fact that the configuration under consideration cannot work in sticking regime with a given input parameters. Unfortunately, that is exactly what happens when $k^{(2)}$ is greater than $k^{(1)}$. In such a situation, it is necessary to choose a different approach when configuring the assumed fields. However, the issues just mentioned are beyond the scope of this paper and can be considered in subsequent studies.

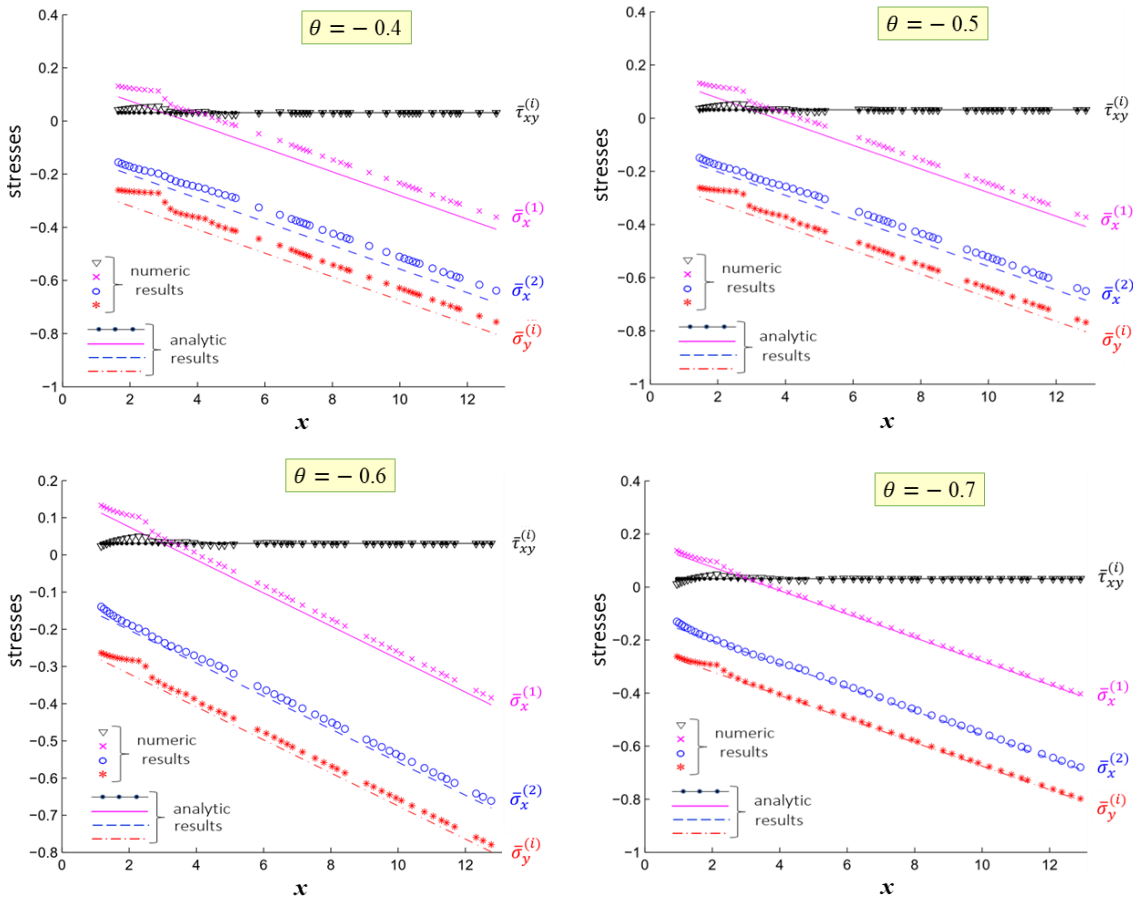

Figure 8. Comparison of numeric and analytic values of $\bar{\sigma}_x^{(1)}$, $\bar{\sigma}_x^{(2)}$, $\bar{\sigma}_y^{(i)}$, $\bar{\tau}_{xy}^{(i)}$ on segment *DG* (The case: $H^{(1)}/H^{(2)} = 0.875$, $k^{(1)}/k^{(2)} = 3$).

6. CONCLUSIONS

A numerical approach based on the method of characteristics for calculating the statically admissible slip-line field of plane-strain compression of a three-layer symmetric strip consisting of two different rigid perfectly plastic materials between rough, parallel, rigid plates has been performed. The numerical results have been evaluated by comparison with an analytic solution which is considered as accurate at the places situated in the distances greater than the strip thickness from the edge of the strip. The approach has been adopted to the case when the shear

yield stress of the inner layer is greater than that of the outer layer ($k^{(1)} > k^{(2)}$). It has been shown that the singularities built at the intersection of rigid-plastic boundary and bi-material interface are necessary to ensure the compatibility of the velocity components at these points and, as a result, the sticking regime on the interface of the strip layers. It should be noted that this will always be true for any other slip-line field configuration when $k^{(1)} \neq k^{(2)}$, as noted in section 3.

Since the construction of a statically admissible slip-line field is the first step in the trial and error process to determine the solutions to the problem in question, the correct configuration set up for these fields and also the possibility of its regulation by suitable determining parameters are of high importance. Therefore the numerical approach presented in the present paper is the first and necessary step to the development of a numerical method for calculating the stress and velocity fields in plane-strain flow of piece-wise homogeneous materials.

Acknowledgements. The research described has been supported by the grants QTRU01.05/18-19 (Vietnam) and RFBR-19-51-52003 (Russia).

Author contributions: Conceptualization, Sergei Alexandrov; Statement of the boundary value problem, Nguyen Manh Thanh; Numerical solution of the problem, Nguyen Trung Kien, Nguyen Manh Thanh.

Declaration of interest conflict: The authors declare that they have no know competing financial interests or personal relationships that could have appeared to influence the work reported in this paper.

REFERENCES

1. Prandtl L. - Anwendungsbeispiele zu einem Henckyschen Salz uber das plastische Gleichgewicht, ZAMM **3** (1923) 401-406.
2. Hill R. - The mathematical theory of plasticity, Clarendon Press, Oxford, 1983.
3. Collins I. F., Meguid S. A. - On the influence of hardening and anisotropy on the plane-strain compression of thin metal strip, Trans. ASME J. Appl. Mech. **44** (1977) 271-278.
4. Adams M. J., Briscoe B. J., Corfield G. M., Lawrence C. J., Papathanasiou T. D. - An analysis of the plane-strain compression of viscoplastic materials, Trans. ASME J. Appl. Mech. **64** (1997) 420-424.
5. Alexandrov S., Mishuris G., Miszuris W. - An analysis of the plane-strain compression of a three-layer strip, Arch. Appl. Mech. **71** (2001) 555-566.
6. Alexandrov S., Tzou G. Y., Huang M. N. - Plane strain compression of a rigid/perfectly plastic multi-layer strip between parallel platens, Acta Mechanica **184** (2006) 103-120.
7. Das N. S., Banerjee J., Collins I. F. - Plane strain compression of rigid perfectly plastic strip between parallel dies with slipping friction, Trans. ASME J. Appl. Mech. **46** (1979) 317-321.
8. Hill R., Lee E. H., Tupper S. J. - A method of numerical analysis of plastic flow in plane strain and its application to the compression of a ductile material between rough plates, Trans. ASME J. Appl. Mech. **18** (1951) 46-52.
9. Alexandrov S., Kuo C. Y., Jeng Y. R. - A Numerical Method for Determining the Strain Rate Intensity Factor Under Plane Strain Conditions, Cont. Mech. Therm. **28** (2015) 977-992.
10. Kachanov L. M. - Foundations of the theory of plasticity, North - Holland Publishing Company, 1971.